IEEE Access
Multidisciplinary | Rapid Review | Open Access Journal

Received June 25, 2020, accepted July 20, 2020, date of publication July 24, 2020, date of current version August 5, 2020.

Digital Object Identifier 10.1109/ACCESS.2020.3011689

Electrical Equipment Identification Method With Synthetic Data Using Edge-Oriented Generative Adversarial Network

ZHEWEN NIU[1], MAREK Z. REFORMAT[2], WENHU TANG[1], (Senior Member, IEEE), AND BAINING ZHAO[1]

[1]School of Electric Power Engineering, South China University of Technology, Guangzhou 510641, China
[2]Department of Electrical and Computer Engineering, University of Alberta, Edmonton T6G 1H9, Canada

Corresponding author: Wenhu Tang (wenhutang@scut.edu.cn)

This work was supported in part by the National Natural Science Foundation of China under Grant 51977082; in part by the Research Project of Qingyuan Power Supply Bureau, Guangdong Power Supply Company Ltd., under Grant GDKJXM20183511; in part by the National Key Research and Development Program of China under Grant 2018YFE0208400; and in part by the China Scholarship Council under Grant 201906150017.

ABSTRACT The fourth industrial revolution – Industry 4.0 – puts emphasis on the application of intelligent technologies in the area of monitoring and identification of electrical equipment. High precision and non-contact qualities make the infrared thermography one of the most suitable technologies for intelligent inspection of high-voltage apparatus. Yet, due to imperfect data acquisition methods and difficulties in collecting data, electrical equipment images are limited in quantities and imbalanced in representing different types of devices. Additionally, it is not easy to extract representative features of infrared images due to their low-intensity contrast and uneven distribution. In this paper, a data-driven framework is proposed for the identification of electrical equipment based on infrared images. The main technique of this proposed system is a novel process of generating synthetic infrared images. For this purpose, an Edge-Oriented Generative Adversarial Network (EOGAN) is developed. The EOGAN is designed to create realistic infrared images that can be used as augmented data for developing data-driven identification methods. Extracted edge features of electrical equipment are utilized as prior information to guide the process of generating realistic infrared images. Finally, comparative experiments are carried out to show the effectiveness of the proposed EOGAN-based framework for equipment identification in the presence of limited and imbalanced image datasets.

INDEX TERMS Edge prior knowledge, electrical equipment identification, generative adversarial network, infrared image.

I. INTRODUCTION

Electrical equipment inspection plays an important role in maintaining safe and reliable operations of power systems. Infrared thermography (IRT), due to its attractive characteristics such as high precision and non-intrusiveness, has become an effective tool in preventive maintenance to ensure safety of electric power systems [1]. Infrared images reveal temperature distributions, based on which the identification and analysis of condition of electrical equipment can be performed [2]. However, the conventional inspection methods are time consuming and require well-qualified and experienced personnel for analyzing images. Therefore, substantial research efforts are focused on the automated methods for effective analysis of electrical equipment based on infrared images.

A fundamental step towards an image-based automatic inspection and diagnosis of equipment is object identification. Conventional identification methods are segmentation-based, which aim at finding the region of interests (ROIs) [3]–[6]. However, these methods identify regions of interest using the hand-crafted features, which are based directly on raw image intensity values and ignore higher-level image representations. With the great success of Convolutional Neural Network (CNN) in computer vision, data-driven methods based on artificial intelligence (AI) gradually become the major research trend in automatic image analysis. AI-based data-driven equipment inspection methods

The associate editor coordinating the review of this manuscript and approving it for publication was Shuaihu Li.

rely on classification and behavior prediction. For instance, Duan *et al.* [7] proposed a fault localization method for transformer internal thermal defects by combining different CNNs and image segmentation methods. Gong *et al.* [8] presented an improved CNN to predict the coordinates, orientation angle, and class type of individual equipment parts. Zhao *et al.* [9] introduced Vector of Locally Aggregated Descriptors (VLAD) to CNNs, which increased robustness of the feature representation and boosted the detection ability of the model.

As known, one of the problems encountered by industrial application of automatic inspection methods is related to actual conditions of acquisition of infrared images. In realistic scenarios, limitations in usefulness of collected data and/or its imbalanced distributions are common [10]. For imbalance datasets, when some types of equipment or problems are hardly captured on images, identification algorithms result in higher classification rates for more 'popular' equipment types but in lower accuracies for the minor ones [11]. Many published literatures have pointed out that data augmentation would function as a regularizer to help improve the performance in the case of imbalanced data distribution [12]–[14]. In the image processing domain, a traditional way is to synthesize data samples using geometric transformations such as translation, scaling, and rotation, as well as channel alterations [15]. However, the data generated in such a way is simple and lacks diversity.

Generative Adversarial Network (GAN) [16] offers an alternative way to address the issue of limited and imbalanced data. It has shown the prominent abilities to generate realistic data [17]. It can be used for data augmentation purposes by generating artificial data that is similar to the original one and thereby enriching a training dataset. The continuous advances in GAN architectures have led to the improvements in quality of image generation and stability of built models. Examples of the improved networks are Deep Convolutional GAN (DCGAN) [18], Wasserstein GAN (WGAN) [19], and Conditional GAN (CGAN) [20]. Many of these models are popular in the domain of industrial applications. Liu *et al.* [21] utilized the synthetic samples generated through GAN from wind turbine data and obtained satisfied fault diagnosis results in the presence of limited data. Wang *et al.* [22] combined WGAN with Stacked De-noising Auto Encoder (SDAE) to perform gearbox fault diagnosis. WGAN was used to expand a number of samples, and SDAE was applied as a classifier to identify signal types. Cabrera *et al.* [23] presented a method that combined Wavelet Packet Transform (WPT) with GAN for building Random Forest (RF) classifiers used for the fault diagnosis of compressors with extremely imbalanced data. Mao *et al.* [24] provided a comparative study and a detailed guidance for applying GANs on imbalanced data for the bearing fault signal diagnosis.

Although the analysis of the aforementioned works indicates a satisfactory performance of fault diagnostic methods using synthetic signals, there is still a lack of investigation of AI-based techniques for data synthesis in the field of object identification when imbalance infrared image datasets are used. In contrast to general identification processes with color images, the infrared images of electrical equipment have their own specific characteristics: 1) they may exhibit over-centralized temperature distribution, i.e., small differences in temperature distribution between pieces of equipment and their environment, resulting in a low intensity contrast; 2) they are captured by hand-held cameras that leads to large variations in the appearance, shape and scale of equipment; and 3) they have complex backgrounds and contain many unrelated objects, which makes the core features of electrical equipment not prominent. Therefore, the infrared images generated by simple application of GAN often lose the main body of the electrical equipment.

To address the above mentioned problems, this paper proposes an Edge-oriented GAN (EOGAN) to generate synthetic infrared images for developing a well performed data-driven electrical equipment identification approach. The extracted features from image edges are utilized as knowledge priors to guide the infrared image generation. These edge priors are beneficial for guiding the infrared thermal image generation process via providing valuable information about boundaries/edges of different types of equipment.

The contributions of this paper are following: 1) proposing a novel weakly supervised method using edge features of objects for generating infrared images of electrical equipment, and implementing it as Edge-oriented Generative Adversarial Network (EOGAN); 2) developing a deep learning based framework for identification of electrical equipment in the presence of small and imbalanced data using the proposed EOGAN for generating synthetic datasets; and 3) conducting extensive experiments using a dataset of real infrared images to illustrate the effectiveness of the proposed EOGAN-based data augmentation framework for equipment identification purposes.

The rest of this paper is organized as follows. Section II is the description of the proposed infrared image generation and electrical equipment identification method. The results of experiments and the discussion are presented in Section III. Finally, Section IV summarizes the conclusion of this paper and a future research plan is given.

II. EQUIPMENT IDENTIFICATION WITH SYNTHETIC DATA

A. ARCHITECTURE OF THE EQUIPMENT IDENTIFICATION METHOD

The main purpose of the proposed method is to generate a large amount of infrared thermal image data in order to provide a sufficient number of samples for the purpose of developing data-driven methods of equipment identification. Yet, there are some challenges related to utilization and processing of infrared thermal images: low resolution and contrast; ambiguous object boundaries caused by a thermal crossover; and a high level of noise introduced by thermal sensors [25].

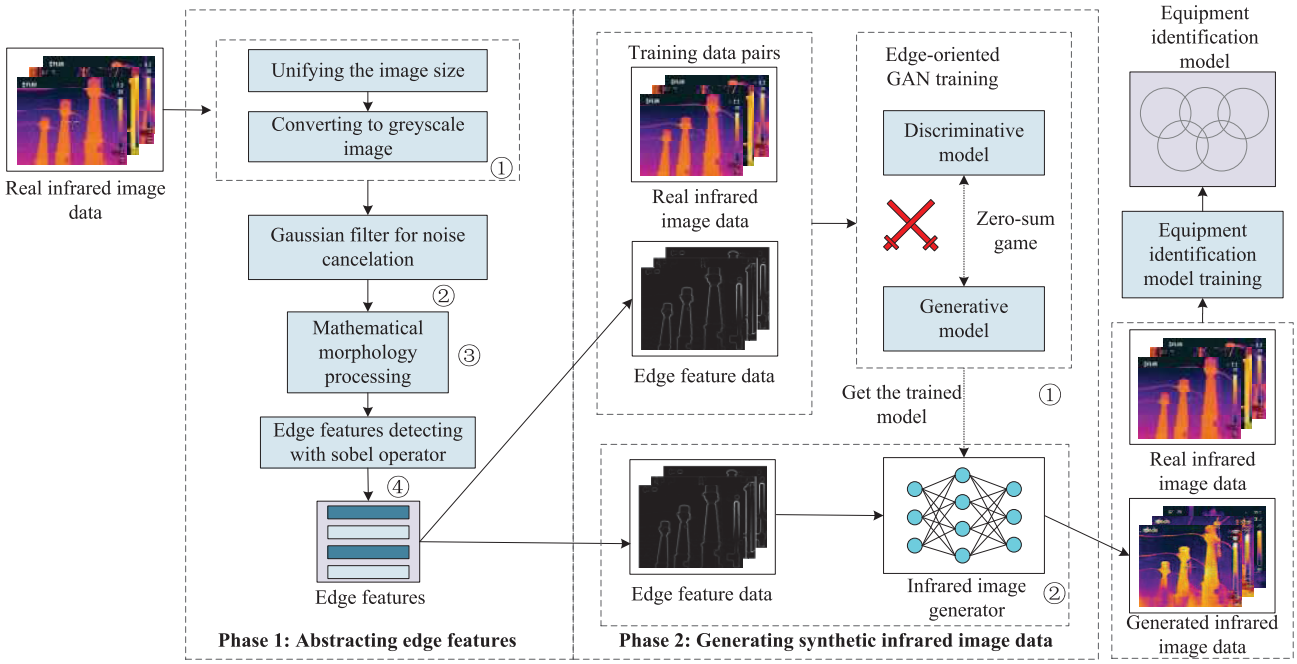

FIGURE 1. Architecture of the proposed electrical equipment identification method.

To handle these problems, we proposed a novel Edge-Oriented GAN. It makes use of edge features to guide a thermal image generation process. Fig. 1 shows the architecture of the proposed method, which consists of three phases.

Phase 1: Abstracting edge information. In this phase, the edge features of infrared thermal images are abstracted in four steps (Fig. 1). In Step 1, the original infrared images are resized and converted into greyscale images. In Step 2, the greyscale images are processed by Gaussian filtering to remove noise and simplify information for subsequent processing. In Step 3, mathematical morphology is utilized to smooth the equipment boundaries and eliminate irrelevant objects such as trees and clouds. Finally, in Step 4, edge features are abstracted using the Sobel edge operator.

Phase 2: Generating synthetic infrared images. In this phase, the EOGAN is constructed and it is used to generated the synthetic infrared images. Two kinds of data are used in this phase: 1) the real infrared image data; and 2) the corresponding edge feature data abstracted from the original infrared image data, *Phase 1*. There are two steps in this phase (Fig. 1). In Step 1, the original real infrared image data and the corresponding edge features are combined to create the training data pairs for constructing the EOGAN. In Step 2, the synthetic infrared image data is generated using the generator of the constructed EOGAN.

Phase 3: Identifying equipment types. Supplemented by a large amount of generated synthetic infrared images, there is a sufficient number of training samples for constructing electrical equipment identification models. Therefore, any data-driven AI method such as CNN can be employed to perform the identification task of equipment types with limited and imbalanced real data samples.

B. EDGE INFORMATION DETECTION

The edge prior knowledge is employed as weakly supervised information to guide the infrared image generation process. In this part, the edge prior knowledge is obtained in four steps. The following sections describe their detailed procedures.

1) RESIZING AND GREYSCALING

Original infrared images may have different picture sizes taken by different cameras. Therefore, image sizes are uniformed to match the size required by the EOGAN. Further, infrared images are converted into greyscale images in order to increase the contracts between bright equipment regions and background regions (Fig. 2(a)). The transformation from the RGB values into the grey values is calculated according to the formula:

$$\text{Grey} = \text{R}^*0.299 + \text{G}^*0.587 + \text{B}^*0.114, \quad (1)$$

where Grey refers to the grey value of a pixel in an infrared image, while R, G, B represent the red, green, and blue values of this pixel, respectively.

2) GAUSSIAN FILTER DENOISING

Gaussian filtering is a linear smoothing filter suitable for eliminating noise and widely used in noise reduction processes. Generally speaking, Gaussian filtering is a process of modifying the entire image via convolution. The value of

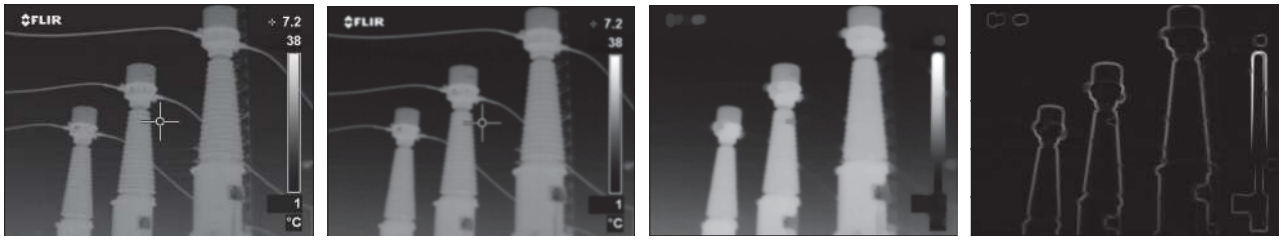

(a) (b) (c) (d)

FIGURE 2. Results of the edge information detection. (a) Greyscaling. (b) Gaussian filter denoising. (c) Mathematical morphology processing. (d) Edge detection with Sobel operator.

each pixel is obtained by using a two-dimensional Gaussian kernel and the weighted average of grey values of pixels in the neighborhood determined by the Gaussian kernel. Here, a specific operation of Gaussian filtering is employed:

$$I_\sigma = I_{\text{gray}} * G_\sigma, \tag{2}$$

where $*$ indicates a convolution operation, I_{gray} represents a greyscale image, and G_σ is a two-dimensional Gaussian kernel with a standard deviation σ, which is defined as:

$$G_\sigma = \frac{1}{2\pi\sigma^2} e^{-(x^2+y^2)/2\sigma^2}, \tag{3}$$

where x, y represent the horizontal and vertical coordinates of the pixel, respectively. A Gaussian smoothing filter is very effective for suppressing noise that obeys normal distribution. The result after Gaussian filter denoising is shown in Fig. 2(b).

3) MATHEMATICAL MORPHOLOGY PROCESSING

Images obtained from the previous processes are rough and contain irrelevant objects, such as trees, clouds, and information about camera's settings. These irrelevant objects can mislead the edge-detection operations and decrease the performance of edge feature extraction methods. Therefore, mathematical morphology is utilized to smooth the contours of objects and to eliminate thin protrusions. Mathematical morphology is a set of nonlinear image processing techniques focused on processing geometric relationships of image pixels [26]. The basic operations of mathematical morphology include dilation, erosion, opening, and closing.

In greyscale morphology, images are functions that map a Euclidean space or grid E into $\mathbb{R} \cup \{\infty, -\infty\}$. Let $f(x, y)$ be a function of an input image while $b(x, y)$ be an operator, the greyscale dilation of $f(x, y)$ by $b(x, y)$ can be defined as:

$$(f \oplus b)(x) = \sup_{y \in E}[f(y) + b(x - y)], \tag{4}$$

where sup denotes the supremum. Similarly, the erosion of $f(x, y)$ by $b(x, y)$ is given by:

$$(f \ominus b)(x) = \inf_{y \in E}[f(y) - b(y - x)], \tag{5}$$

where inf refers to the infimum. Here, the greyscale opening operation is applied to eliminate glitches and highlight edge information of electrical equipment. The greyscale opening operation is obtained by the erosion of $f(x, y)$ by $b(x, y)$, followed dilation by $b(x, y)$:

$$f \circ b = (f \ominus b) \oplus b. \tag{6}$$

An example of such operation is shown in Fig. 2(c).

4) EDGE DETECTION USING THE SOBEL OPERATOR

In this step, the process of edge detection of electrical equipment is implemented using the Sobel edge detection algorithm. Sobel edge detection is a widely used algorithm of edge detection in image processing [27]. The Sobel operator performs a 2-D spatial gradient measurement on an image and so emphasizes regions of high spatial frequency that correspond to edges. Typically, it is used to find the approximate absolute gradient magnitude at each point of an input greyscale image. In this study, the Sobel edge detection algorithm is chosen, as it is convenient and fast and its performance is good. It is especially true due to the fact that noise and glitches that affect the accuracy of the Sobel algorithm are eliminated in the previous steps.

The Sobel operator consists of a pair of 3×3 convolution masks, which are defined as (7):

$$\begin{bmatrix} -1 & 0 & 1 \\ -2 & 0 & 2 \\ -1 & 0 & 1 \end{bmatrix} \quad \text{and} \quad \begin{bmatrix} -1 & -2 & -1 \\ 0 & 0 & 0 \\ 1 & 2 & 1 \end{bmatrix}. \tag{7}$$

Generally, the masks are applied separately to the input image and produce separate measurements of the gradient components in each orientation, i.e., vertically and horizontally. Further, they are combined to determine the absolute gradient magnitude of each point. In this way, the edge features of electrical equipment are obtained, Fig. 2(c). The four-step edge detection method has the following advantages: 1) it is suitable for handling different types of infrared images captured by different infrared camera; 2) it can effectively extract edge features of electrical equipment from infrared images with a complex background; and 3) it is easy to implement and has a fast execution. In the next section, the extracted edge features are used as prior knowledge to train GAN.

C. GENERATION OF SYNTHETIC INFRARED IMAGE

In this section, an Edge-Oriented GAN is developed to generate synthetic infrared images. The edge information of electrical equipment is utilized to guide the generation of infrared images to maintain clear boundaries of electrical equipment.

1) GENERATIVE ADVERSARIAL NETWORK

Generative adversarial network (GAN) consists of two networks, i.e., a generator G and a discriminator D, both competing against each other. The main reason to use GAN is that adversarial networks can improve the quality of generated data. The purpose of G is to generate synthetic samples that should be almost indistinguishable from the real ones, while the aim of D is to try to discriminate if samples (images) are real or fake.

In particular, the input to G is a set of random noise z sampled from a distribution p_z. The output of G is the synthetic samples $G(z) \sim p_g$, where p_g represents the distribution of $G(z)$. The input to D is a real data sample x with distribution p_r, or the synthetic samples $G(z)$ generated by G. In theory, $D(x) = 1$ if $x \sim p_r$ and $D(x) = 0$ if $x \sim p_g$. The training process is a minimax two-player game with an objective function as follows:

$$\min_G \max_D V(D,G) = \min_G \max_D \left(\mathbb{E}_{x\sim p_r(x)} \log D(x) + \mathbb{E}_{z\sim p_z(z)} \log(1 - D(G(z)))\right), \quad (8)$$

where the first summand improves the model's ability to detect real inputs and the second summary improves the model's ability to recognize inputs generated by G. During the training process, G and D are trained alternately until the Nash equilibrium is reached.

2) EDGE-ORIENTED GAN

Theoretically, GAN is able to generate images using a series of random noise signals. However, in practice, due to the fact that there is no control on how the data being generated, the complexity of the infrared image background and existence of many elements on the image means that GANs tend to fall into the problem of non-convergence. Conditional GAN (CGAN) is a promising version of GAN which is designed to generate fake samples with specific conditions or characteristics rather than generic samples from unknown noise distribution. Generally, the conditional information of CGAN could be a label associated with an image or a more detailed tag [28].

Inspired by the CGAN, the proposed Edge-Oriented GAN (EOGAN) is developed utilizing the equipment edge features of infrared images as the conditional information to guide the process of generating infrared images of electrical equipment.

The development of the EOGAN follows the process of supervised learning. First, the original infrared images x and the associated edge feature data y are combined to constitute a set of original data pairs. Then, the infrared images $G(z|y)$ generated by the generator G are combined together

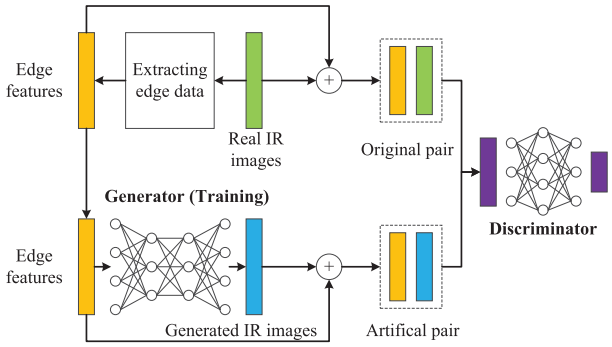

FIGURE 3. The proposed EOGAN-based infrared image generator: training process.

the edge features y as generated data pairs. Finally, both the original data pairs and the generated data pairs are used as the input to discriminator D. The details of the training process of EOGAN are shown in Fig. 3. The loss function of the discriminator D is listed as follows:

$$L^{(D)}_{\text{EOGAN}}\left(\theta^{(G)}, \theta^{(D)}\right) = -\mathbb{E}_{x-p_{\text{data}}} \log D(x|y) - \mathbb{E}_z \log\left(1 - D\left(G\left(z|y\right)\right)\right). \quad (9)$$

In every training iteration of the discriminator D, the parameters of discriminator $\theta^{(D)}$ are updated using the stochastic gradient $\nabla_{\theta_D} L_{\text{EOGAN}}(D)$. After updating $\theta^{(D)}$, the loss of generator $L_{\text{EOGAN}}(G)$ is calculated. According to (9), the loss function of the generator is described as follows:

$$L^{(G)}_{\text{EOGAN}}\left(\theta^{(G)}, \theta^{(D)}\right) = -\mathbb{E}_z \log D\left(G\left(z|y\right)\right). \quad (10)$$

In order to make the generated infrared images a better approximation of the real ones, a traditional loss L_{tra} is added in the loss function of generator. In this study, L1 distance is chosen as the traditional loss:

$$L_{\text{L}\,1}(G) = \mathbb{E}_{x,y,z}\|x - G(y,z)\|_1. \quad (11)$$

Therefore, the generator's task is not only to deceive the discriminator but also to be close to the output ground truth. After adding the traditional loss, the loss function of the generator is described as belows:

$$\begin{aligned} L^{(G)}_{\text{EO}}\left(\theta^{(G)}, \theta^{(D)}\right) &= L^{(G)}_{\text{EOGAN}} + \lambda_{\text{L}\,1}(G) \\ &= -\mathbb{E}_z \log D\left(G\left(z|y\right)\right) \\ &\quad + \lambda \mathbb{E}_{x,y,z}\|x - G(y,z)\|_1. \end{aligned} \quad (12)$$

Next, the parameters of generator, $\theta^{(G)}$, are updated by using the stochastic gradient $\nabla_{\theta_D} L_{\text{EO}}(G)$. Finally, the EOGAN-based infrared image generator is trained by updating the parameters of $\theta^{(D)}$ and $\theta^{(G)}$ alternately. To sum up, in order to closely reflect characteristics of original infrared images and generate more realistic ones, the proposed EOGAN makes the following improvements on the basis of CGAN: 1) Edge features are utilized as the conditional information to supervise the generating process of the generator; 2) A traditional loss is added to the generator.

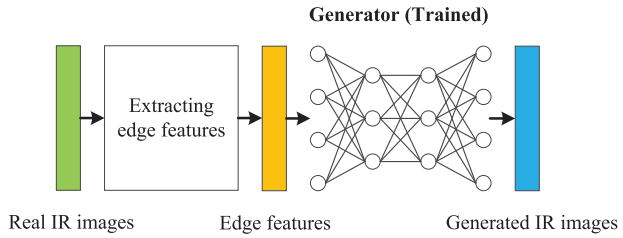

FIGURE 4. The proposed EOGAN-based infrared image generator: generating process.

With the proposed EOGAN, the generator can produce images possessing clear subject features of the original ones.

3) GENERATING ELECTRICAL EQUIPMENT INFRARED IMAGES

In this procedure, the edge features of electrical equipment determined in *Phase 1* are used for generating synthetic infrared images. The EOGAN-based generator can generate infrared images of electrical equipment according to the edge information. The process of generating synthetic infrared images is illustrated in Fig. 4. Consequently, a sufficient number of infrared images can be supplied for constructing the data-driven AI methods for electrical equipment identification.

D. IDENTIFICATION OF ELECTRICAL EQUIPMENT TYPES

In this study, a data-driven deep learning model is developed to identify types of electrical equipment based on infrared images. Convolutional neural networks (CNNs) are utilized as the deep feature extractor due to their remarkable effectiveness in all kinds of computer vision tasks [29]. Besides, given the shortage of data samples in practical applications, transfer learning [30] is adopted to reduce the computational burden. The flowchart of the electrical equipment infrared image identification is shown in Fig. 5.

As presented in Fig. 5, the VGG16 architecture released by [31] is employed. This allows for achieving the state-of-the-art accuracy for many classification tasks. Additionally, instead of optimizing the whole model on the limited dataset, an ImageNet pre-trained VGG16 model is adopted to extract deep feature maps. The real infrared images and the generated synthetic images are put (combined) together as the input dataset. Features located at the last pooling layer are used as the feature vectors. In this study, the input image size is 224×224, and the obtained feature vectors are of size $7 \times 7 \times 512$. Finally, the identification probabilities are calculated by classifiers.

III. EXPERIMENTS AND DISCUSSION

In order to evaluate the ability of EOGAN-based data synthesis scheme to improve the performance of equipment identification accuracy, two comparative experiments are designed. *Experiment 1* is a verification experiment focused on the performance in the presence of imbalanced data. The target

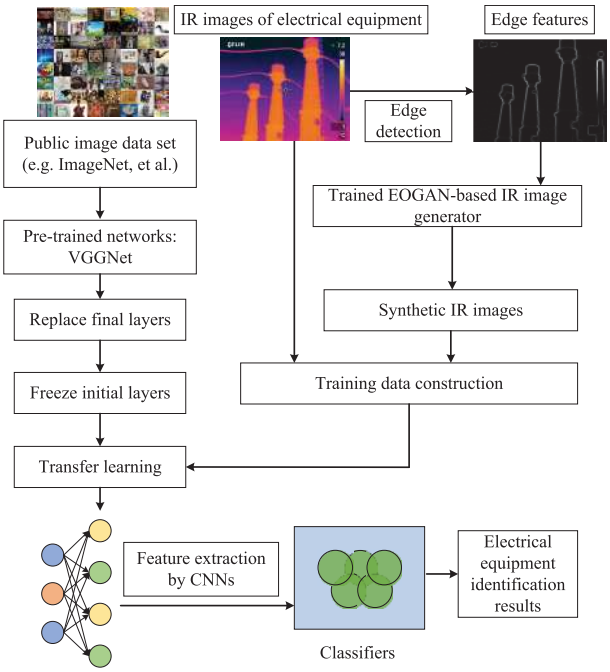

FIGURE 5. Flowchart of the electrical equipment IR image identification.

is to investigate the influence of the quantity of generated synthetic images on the classification accuracy. Different testing scenarios with a different number of generated images, as well as different types of classifiers are explored here.

Experiment 2 is designed based on the results of *Experiment 1*. This experiment investigates the influence of the proposed method on classification results in the case when the imbalanced training data is supplemented by the generated infrared images. Numbers of samples from 'small' categories are increased by adding images generated by the proposed EOGAN. In *Experiment 2*, four commonly used balancing methods are applied to illustrate effectiveness of the proposed method.

A. DATASET AND EVALUATION METRICS

In this study, we use the infrared image dataset that contains images of electrical equipment collected during the inspection of a power grid. The dataset contains infrared images of five electrical devices. Yet, the numbers of images per a single type of equipment are different. Specifically, the dataset includes 244 arresters, 214 breakers, 302 current transformers, 428 potential transformers, and 112 Y-shape breakers, a total of 1050 infrared images.

A few typical samples of different equipment types are shown in Fig. 6. It can be seen that infrared images of electrical equipment have the following characteristics: 1) a variety of pseudo-colors are present; 2) various pieces of information such as the trademark, aiming frame, temperature values produced by the infrared camera are superimposed on the images; 3) the image backgrounds are complex; and 4) there are multiple shooting angels of the thermal imaging camera.

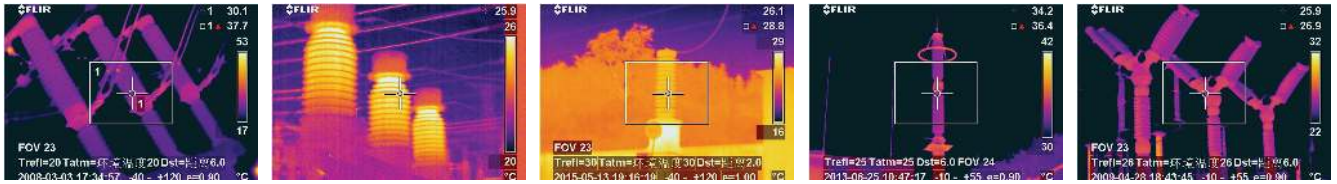

(a) (b) (c) (d) (e)

FIGURE 6. Typical samples of infrared image dataset. (a) Breaker. (b) Current transformer (CT). (c) potential transformer (PT). (d) Arrester. (e) Y-shape breaker.

For the experiments, the dataset is divided into a training set and a test set in the proportion of 8:2. In order to ensure the confidence of the presented results, the generated images are only added to the training set, while the test set is composed of the real samples all the time.

In this research, the performance is evaluated based on accuracy, precision, recall, and F1-score, which are given as:

$$\text{Accuracy} = \frac{TP + TN}{TP + FP + TN + FN} \tag{13}$$

$$\text{Precision} = \frac{TP}{TP + FP} \tag{14}$$

$$\text{Recall} = \frac{TP}{TP + FN} \tag{15}$$

$$\text{F1-score} = \frac{2 \times \text{precision} \times \text{recall}}{\text{precision} + \text{recall}}. \tag{16}$$

Accuracy is the proportion of a total of correctly identified equipment samples over the entire tested samples. Precision is a function of the correctly classified samples (true positives) and examples misclassified as positives (false positives). Recall is a function of the true positives and the misclassified samples (false negatives). F1-score is a measure combining both recall and precision.

B. EXPERIMENT 1

This experiment focuses on evaluating the performance of the proposed EOGAN-based image synthesis method. Datasets of different sizes are created via adding generated synthetic images into the original dataset. Created datasets are used to construct a number of electrical equipment identification models and compare their classification results.

The EOGAN-based model is trained using the procedure shown in Fig. 3. When the value of loss function of the discriminator converges and falls into a low value range, the synthetic images generated by EOGAN are considered as of high quality. Fig. 7 contains a few samples of such images.

It is clear from Fig. 7 that the generated synthetic infrared images look realistically and are similar to the real images. Both shapes and boundaries of the electrical equipment are well presented on the generated synthetic images. However, the generated images are not exactly the same as the original ones, and there exist some small differences. Small divergences between the synthetic images and the real ones are acceptable and even wished for. Such small differences would improve the robustness of constructed image identification models and enhance their generalization ability as well, and this is verified in *Experiment 2*.

FIGURE 7. Synthetic infrared images generated by the EOGAN-base image augmentation method.

In order to check the impact of synthetic images on the identification accuracy, different numbers of synthetic images for each equipment type are added to the training set. In addition, various commonly used classifiers are investigated, i.e., Softmax function, random forest (RF) classifier, and support vector machine (SVM). Since the main purpose of this experiment is to explore the ability of EOGAN-based augmentation to help classification tasks, it is worth to mention that the parameters of the classifiers are all set to the default ones without any optimizations. Note that we are not balancing the dataset in this experiment, the new training set is still imbalanced after adding the same number of synthetic images to each category. To make a more reliable comparison, the mean value of 10 trials are taken as the final results, as illustrated in Table 1 and Table 2.

Fig. 8 and Fig. 9 show the results of the identification accuracy with a different number of synthetic images added per class. It can be observed, Fig. 8, that the identification accuracy of all three classifiers increases with the increasing number of added synthetic images. It demonstrates that the generated synthetic images can provide useful information and lead to improvements in the performance of data-driven equipment identification models. Specifically, the Softmax function delivers the best identification performance. If the accuracy of 0.90 is taken as a threshold, the Softmax function needs 30 synthetic images to reach it, while SVM needs 190 and RF needs approximately 600. From the perspective of

TABLE 1. Experiment 1: accuracy versus the number of synthetic samples added per class with different classifiers.

Accuracy	0	100	200	300	400	600	800
Softmax	0.877±0.021	0.931±0.019	0.941±0.016	0.947±0.008	0.962±0.007	0.976±0.006	0.978±0.004
SVM	0.821±0.110	0.886±0.046	0.910±0.046	0.925±0.020	0.933±0.018	0.958±0.015	0.967±0.014
RF	0.749±0.062	0.790±0.056	0.833±0.041	0.858±0.045	0.883±0.029	0.904±0.032	0.922±0.028

TABLE 2. Experiment 1: F1-score versus different number of synthetic samples added per class with different classifiers.

F1-score	0	100	200	300	400	600	800
Softmax	0.871±0.025	0.928±0.017	0.940±0.015	0.943±0.010	0.961±0.008	0.974±0.007	0.977±0.005
SVM	0.820±0.114	0.887±0.047	0.911±0.041	0.927±0.020	0.935±0.017	0.961±0.018	0.968±0.017
RF	0.634±0.102	0.781±0.063	0.836±0.039	0.861±0.041	0.887±0.027	0.907±0.033	0.924±0.027

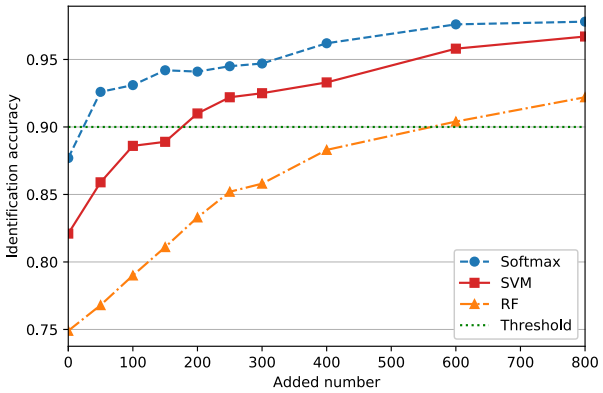

FIGURE 8. Identification accuracy of Experiment 1 with different number of synthetic images added per class.

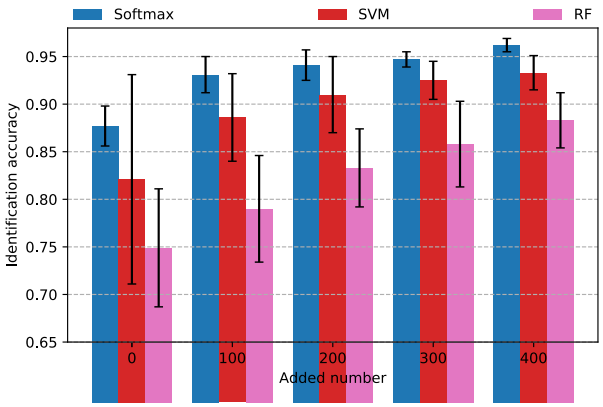

FIGURE 9. Identification accuracy of Experiment 1 with different number of synthetic images added per class.

stability of performance, Fig. 9, the values of standard derivation show a downward trend once the synthetic images are added. The Softmax function obtains the best classification stability compared with the other two classifiers. In addition, Table 2 lists the F1-score values, which indicates that both the precision and recall are improved after adding the synthetic images.

C. EXPERIMENT 2

In real scenarios, the collected infrared images of electrical equipment are predominantly imbalanced. This fact alone has a negative effect on the identification accuracies of prediction models. In order to investigate the effectiveness of the proposed EOGAN-based data augmentation method in alleviating the problem of imbalanced training data, several comparative tests are designed and their results are presented here.

Synthetic images generated by the proposed EOGAN-based data augmentation method can be treated as supplement samples to an imbalanced training dataset. In *Experiment 2*, a number of added samples vary between categories of the equipment – only so many of them are added to obtain a balanced dataset.

This also allows us to learn how good the generated images are via observing the performance of classifiers constructed using data, where some classes have more synthetic images than the real ones. Based on the results of *Experiment 1*, the Softmax function is selected as the classifier due to its good performance in both accuracy and stability.

To evaluate the effectiveness of the EOGAN method in helping deal with imbalanced data, synthetic data generated by EOGAN are added to the minor classes to create a balanced dataset. Therefore, the number of added samples of each type of equipment aims to achieve that all the classes have the same number of samples – 428 (the size of the largest class of potential transformers). The classification performance of the models built based on the original imbalanced training data and the one built on the balanced data is shown in Fig. 10 and Fig. 11, respectively. It can be seen, Fig. 10, that the model built based on the balanced data – achieved by adding images generated using the proposed method – has a higher identification accuracy. Fig. 11 shows the confusion matrices of the original model – built based on the imbalanced training set – and the confusion matrix of the model built using the balanced data. The improvement in the identification performance (for each type of equipment) is class. This indicates the effectiveness of the proposed EOGAN to generate synthetic samples for tackling the problem of imbalanced dataset.

For further comparison, the proposed method is compared with other widely-used image dataset balancing methods, such as Random Oversampling (RO) [15],

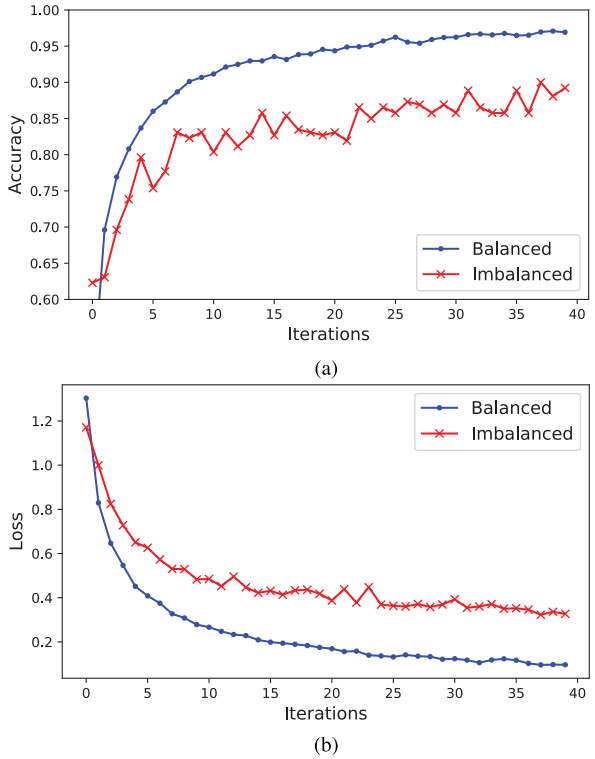

FIGURE 10. Comparative results of the proposed method for imbalanced vs. balanced training data in terms of (a) Classification accuracy. (b) Classification loss.

TABLE 3. Comparative results of identification accuracy using different balancing methods.

Accuracy	CT	PT	Breaker	Arrester	Y-breaker
RO	0.972	0.954	0.941	0.974	0.958
U	0.870	0.862	0.846	0.894	0.804
DCGAN	0.981	0.952	0.918	0.981	0.952
WGAN	0.980	0.954	0.915	0.983	0.974
EOGAN	0.992	0.980	0.959	0.989	0.996

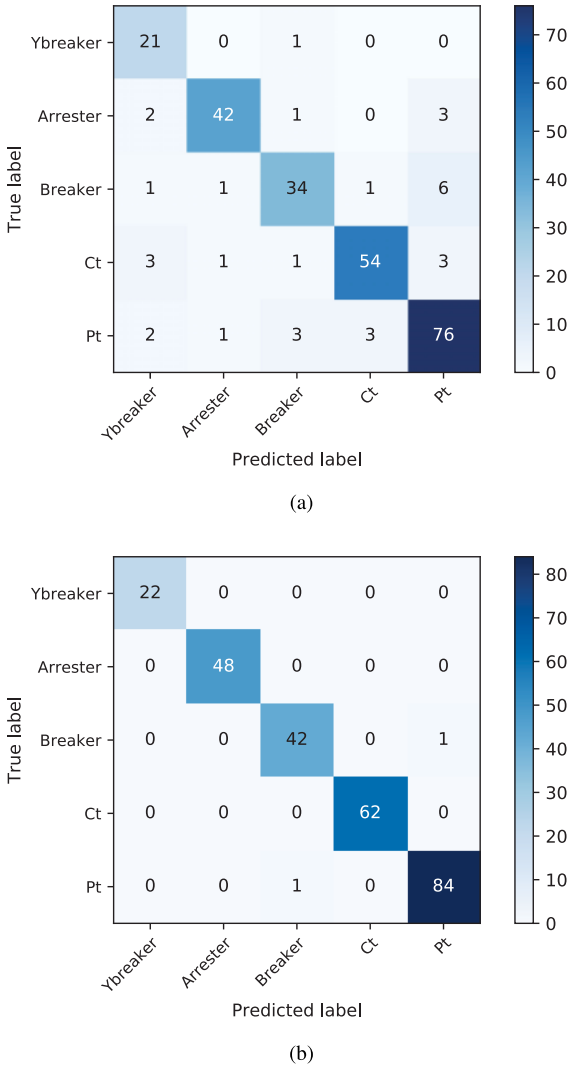

FIGURE 11. The confusion matrices of (a) Original imbalanced training set. (b) Balanced training set.

Undersampling (U) [32] and two popular GANs: DCGAN and WGAN. RO uses geometric transformations for randomly selected images to supplement a training set until the balance is reached. While U randomly selects images of the majority set to be eliminated until the balance of the entire dataset is reached. Therefore, the number of samples of each type of equipment reaches 428 for RO, DCGAN, WGAN, and EOGAN, while for the case of U the number is 112 images for each type – a size of the smallest category of Y-shape breakers. To ensure sound results, the reported values are the means of 10 repeated trials, Table 3.

It can be seen that the proposed EOGAN leads to the best identification performance for every type of electrical equipment, when compared with the other four data balancing methods. Particularly, the proposed EOGAN obtains a better performance than RO. This indicates that the dataset augmented by the EOGAN contains more diversity than the simple duplication of images, which can improve the robustness and generalization ability of an AI-based data-driven model.

To show the confidence in the obtained comparative results, the T-student test is used to calculate the statistical significance between the results obtained with the EOGAN and the other four balancing methods. The p-values of the T-student test are listed in Table 4, which are less than 0.001, and indicates the existence of significant difference between the identification accuracy of EOGAN-based method when compared to the four balancing methods. Therefore, it can be deduced that the synthetic infrared images generated by EOGAN are helpful in dealing with imbalanced training data for electrical equipment identification.

In addition, to further investigate the effectiveness of the EOGAN as a data balancing method, another comparison is designed. In this comparison, the number of samples of each type of equipment is set as 428, while the number of real images among them is varied. Firstly, only 25% of original images in each class is used, then we increase it to 50%, and finally all the available real images are employed – 100%. In each of these cases, a number of generated images is such

TABLE 4. The p-values of T-student test between the results of EOGAN and the other four balancing methods.

P-value	CT	PT	Breaker	Arrester	Y-breaker
RO	0.0001	2.99E-05	0.0004	0.0001	3.31E-05
U	2.16E-09	6.83E-10	9.90E-12	1.20E-09	2.74E-010
DCGAN	1.43E-07	3.01E-06	4.33E-08	8.13E-07	1.55E-08
WGAN	1.60E-11	2.54E-09	5.94E-11	4.51E-11	6.10E-10

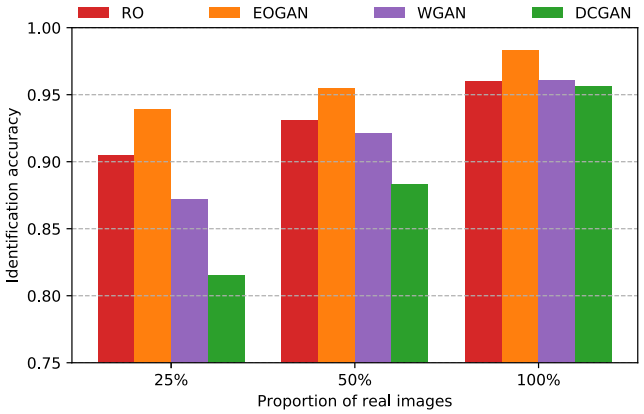

FIGURE 12. Identification accuracy using different proportion of available real samples.

that the total number of samples in each class equals to 428. In this part, the comparison is done against RO, WGAN, and DCGAN.

Fig. 12 demonstrates the result of this comparison. It indicates that: 1) the proposed EOGAN-based data augmentation method is effective in dealing with imbalanced classification problems even when the available real data is limited; 2) when the number of available real data is very low, RO could suffer from the over-fitting problem; and 3) it is difficult for DCGAN and WGAN to capture useful information from infrared images under a limited data situation, while the edge prior knowledge in the EOGAN can alleviate this problem to some extent.

IV. CONCLUSION

In this paper, an EOGAN-based data-driven identification framework for electrical equipment has been proposed using a process of generating synthetic images. In order to produce high-quality synthetic samples, edge features of electrical equipment are extracted as weakly supervised information to guide the infrared image generation process. Generated artificial samples enable solving the problem of limited and imbalanced data when training an AI-based data-driven model. In addition, the presented comparative experiments using real infrared image datasets confirm the effectiveness of the proposed method.

Based on the experimental results, the following conclusions are drawn: 1) the proposed EOGAN-based method is an effective data augmentation technique for building data-driven identification models; 2) when compared with the widely-used data balancing techniques, the EOGAN not only generates synthetic samples of better quality but also possesses a higher diversity; 3) the constructed framework for identification of electrical equipment provides a very satisfactory performance, when the proposed EOGAN-based method to mitigate the problem of imbalance dataset is used; and 4) the synthetic data generated by the proposed method still leads to a high identification accuracy, even when the number of real data samples is very small.

In the future, the authors will focus on improving the EOGAN-based data augmentation scheme to enable the development of equipment fault diagnostic systems when only small datasets are available.

REFERENCES

[1] S. Bagavathiappan, B. B. Lahiri, T. Saravanan, J. Philip, and T. Jayakumar, "Infrared thermography for condition monitoring—A review," *Infr. Phys. Technol.*, vol. 60, pp. 35–55, Sep. 2013.

[2] Y. Tu, B. Gong, C. Wang, K. Xu, Z. Xu, S. Wang, F. Zhang, and R. Li, "Effect of moisture on temperature rise of composite insulators operating in power system," *IEEE Trans. Dielectr. Electr. Insul.*, vol. 22, no. 4, pp. 2207–2213, Aug. 2015.

[3] Z. Zhao, N. Liu, and L. Wang, "Localization of multiple insulators by orientation angle detection and binary shape prior knowledge," *IEEE Trans. Dielectr. Electr. Insul.*, vol. 22, no. 6, pp. 3421–3428, Dec. 2015.

[4] M. S. Jadin, S. Taib, and K. H. Ghazali, "Finding region of interest in the infrared image of electrical installation," *Infr. Phys. Technol.*, vol. 71, pp. 329–338, Jul. 2015.

[5] H. Zou and F. Huang, "A novel intelligent fault diagnosis method for electrical equipment using infrared thermography," *Infr. Phys. Technol.*, vol. 73, pp. 29–35, Nov. 2015.

[6] Z. Zhao, G. Xu, and Y. Qi, "Representation of binary feature pooling for detection of insulator strings in infrared images," *IEEE Trans. Dielectr. Electr. Insul.*, vol. 23, no. 5, pp. 2858–2866, Oct. 2016.

[7] J. Duan, Y. He, B. Du, R. M. R. Ghandour, W. Wu, and H. Zhang, "Intelligent localization of transformer internal degradations combining deep convolutional neural networks and image segmentation," *IEEE Access*, vol. 7, pp. 62705–62720, 2019.

[8] X. Gong, Q. Yao, M. Wang, and Y. Lin, "A deep learning approach for oriented electrical equipment detection in thermal images," *IEEE Access*, vol. 6, pp. 41590–41597, 2018.

[9] Z. Zhao, X. Fan, G. Xu, L. Zhang, Y. Qi, and K. Zhang, "Aggregating deep convolutional feature maps for insulator detection in infrared images," *IEEE Access*, vol. 5, pp. 21831–21839, 2017.

[10] F. Jia, Y. Lei, N. Lu, and S. Xing, "Deep normalized convolutional neural network for imbalanced fault classification of machinery and its understanding via visualization," *Mech. Syst. Signal Process.*, vol. 110, pp. 349–367, Sep. 2018.

[11] I. Martin-Diaz, D. Morinigo-Sotelo, O. Duque-Perez, and R. de J. Romero-Troncoso, "Early fault detection in induction motors using AdaBoost with imbalanced small data and optimized sampling," *IEEE Trans. Ind. Appl.*, vol. 53, no. 3, pp. 3066–3075, May 2017.

[12] X. Zhu, Y. Liu, Z. Qin, and J. Li, "Data augmentation in emotion classification using generative adversarial networks," 2017, *arXiv:1711.00648*. [Online]. Available: http://arxiv.org/abs/1711.00648

[13] K. He, X. Zhang, S. Ren, and J. Sun, "Deep residual learning for image recognition," in *Proc. IEEE Conf. Comput. Vis. Pattern Recognit. (CVPR)*, Jun. 2016, pp. 770–778.

[14] X. Gao, F. Deng, and X. Yue, "Data augmentation in fault diagnosis based on the Wasserstein generative adversarial network with gradient penalty," *Neurocomputing*, vol. 396, pp. 487–494, Jul. 2020.

[15] S. C. Wong, A. Gatt, V. Stamatescu, and M. D. McDonnell, "Understanding data augmentation for classification: When to warp?" in *Proc. Int. Conf. Digit. Image Comput., Techn. Appl. (DICTA)*, Nov./Dec. 2016, pp. 1–6.

[16] I. J. Goodfellow, J. Pouget-Abadie, M. Mirza, B. Xu, D. Warde-Farley, S. Ozair, A. Courville, and Y. Bengio, "Generative adversarial nets," in *Proc. Int. Conf. Neural Inf. Process. Syst.*, vol. 3, 2014, pp. 2672–2680.

[17] S. Shao, P. Wang, and R. Yan, "Generative adversarial networks for data augmentation in machine fault diagnosis," *Comput. Ind.*, vol. 106, pp. 85–93, Apr. 2019.
[18] A. Radford, L. Metz, and S. Chintala, "Unsupervised representation learning with deep convolutional generative adversarial networks," 2015, *arXiv:1511.06434*. [Online]. Available: http://arxiv.org/abs/1511.06434
[19] I. Gulrajani, F. Ahmed, M. Arjovsky, V. Dumoulin, and A. C. Courville, "Improved training of Wasserstein GANs," in *Proc. Adv. Neural Inf. Process. Syst.*, 2017, pp. 5767–5777.
[20] P. Isola, J.-Y. Zhu, T. Zhou, and A. A. Efros, "Image-to-Image translation with conditional adversarial networks," in *Proc. IEEE Conf. Comput. Vis. Pattern Recognit. (CVPR)*, Jun. 2017, pp. 5967–5976.
[21] J. Liu, F. Qu, X. Hong, and H. Zhang, "A small-sample wind turbine fault detection method with synthetic fault data using generative adversarial nets," *IEEE Trans. Ind. Informat.*, vol. 15, no. 7, pp. 3877–3888, Jul. 2019.
[22] J. Wang, S. Li, B. Han, Z. An, H. Bao, and S. Ji, "Generalization of deep neural networks for imbalanced fault classification of machinery using generative adversarial networks," *IEEE Access*, vol. 7, pp. 111168–111180, 2019.
[23] D. Cabrera, F. Sancho, J. Long, R.-V. Sánchez, S. Zhang, M. Cerrada, and C. Li, "Generative adversarial networks selection approach for extremely imbalanced fault diagnosis of reciprocating machinery," *IEEE Access*, vol. 7, pp. 70643–70653, 2019.
[24] W. Mao, Y. Liu, L. Ding, and Y. Li, "Imbalanced fault diagnosis of rolling bearing based on generative adversarial network: A comparative study," *IEEE Access*, vol. 7, pp. 9515–9530, 2019.
[25] C. Li, W. Xia, Y. Yan, B. Luo, and J. Tang, "Segmenting objects in day and night: Edge-conditioned CNN for thermal image semantic segmentation," 2019, *arXiv:1907.10303*. [Online]. Available: http://arxiv.org/abs/1907.10303
[26] J.-Y. Lu, H.-P. Pan, and Y.-M. Xia, "The weld image edge-detection algorithm combined with Canny operator and mathematical morphology," in *Proc. 32nd Chin. Control Conf.*, 2013, pp. 4467–4470.
[27] Y. Zhang, X. Han, H. Zhang, and L. Zhao, "Edge detection algorithm of image fusion based on improved Sobel operator," in *Proc. IEEE 3rd Inf. Technol. Mechatronics Eng. Conf. (ITOEC)*, Oct. 2017, pp. 457–461.
[28] J. Gauthier, "Conditional generative adversarial nets for convolutional face generation," *Class Project Stanford CS231N, Convolutional Neural Netw. Vis. Recognit., Winter semester*, vol. 2014, no. 5, p. 2, 2014.
[29] M. Oquab, L. Bottou, I. Laptev, and J. Sivic, "Learning and transferring mid-level image representations using convolutional neural networks," in *Proc. IEEE Conf. Comput. Vis. Pattern Recognit. (CVPR)*, Jun. 2014, pp. 1717–1724.
[30] B. Zhao, B. Huang, and Y. Zhong, "Transfer learning with fully pretrained deep convolution networks for land-use classification," *IEEE Geosci. Remote Sens. Lett.*, vol. 14, no. 9, pp. 1436–1440, Sep. 2017.
[31] K. Simonyan and A. Zisserman, "Very deep convolutional networks for large-scale image recognition," 2014, *arXiv:1409.1556*. [Online]. Available: http://arxiv.org/abs/1409.1556
[32] J. Hernandez, J. A. Carrasco-Ochoa, and J. F. Martinez-Trinidad, "An empirical study of oversampling and undersampling for instance selection methods on imbalance datasets," in *Progress in Pattern Recognition, Image Analysis, Computer Vision, and Applications* (Lecture Notes in Computer Science). Berlin, Germany: Springer, 2013, pp. 262–269.

ZHEWEN NIU received the B.Sc. degree in electrical engineering from the Taiyuan University of Technology, Taiyuan, China, in 2016. He is currently pursuing the Ph.D. degree in electrical engineering with the South China University of Technology, Guangzhou, China. He is also with the Department of Electrical and Computer Engineering, University of Alberta, Alberta, Canada, as a Visiting Scholar under the support of China Scholarship Council (CSC). His research interests include deep learning and data mining in power systems.

MAREK Z. REFORMAT received the M.Sc. degree (Hons.) from the Technical University of Poznan, Poland, and the Ph.D. degree from the University of Manitoba, Canada.

He is currently a Full Professor at the Department of Electrical and Computer Engineering, University of Alberta. His research interest includes the development of methods and techniques for intelligent data modeling and analysis leading to translation of data into knowledge. He uses the concepts of computational intelligence with fuzzy computing and possibility theory in particular machine learning and knowledge discovery as key elements necessary for capturing relationships between pieces of data and knowledge, and for introducing human aspects to data analysis and decision-making processes resulting in more human-aware and human-like systems. He has published peer-reviewed publications in the areas of computational intelligence, knowledge, and software engineering.

He is an Associate Editor of a number of international journals. He is the past President of the North American Fuzzy Information Processing Society (NAFIPS) and the President of the International Fuzzy Systems Association (IFSA).

WENHU TANG (Senior Member, IEEE) received the B.Sc. and M.Sc. degrees in electrical engineering from the Huazhong University of Science and Technology, Wuhan, China, in 1996 and 2000, respectively, and the Ph.D. degree in electrical engineering from the University of Liverpool, Liverpool, U.K., in 2004. He was a Postdoctoral Research Associate and subsequently a Lecturer at the University of Liverpool, from 2004 to 2013. He is currently a Distinguished Professor and the Dean of the School of Electric Power Engineering, South China University of Technology, Guangzhou, China. He has authored and coauthored 150 research articles, including 60 international journal articles and one monograph in Springer. His research interests include power systems risk assessment, renewable energy integration in power grids, condition monitoring and fault diagnosis for power apparatus, multiple-criteria evaluation, and intelligent decision support systems. He is a Fellow of IET.

BAINING ZHAO received the B.Sc. degree in electrical engineering from the South China University of Technology, Guangzhou, China, in 2019, where he is currently pursuing the M.Sc. degree. His research interests include deep learning, fault diagnosis, and wind energy.